A Calibration of the MeteoSwiss RAman Lidar for Meteorological Observations (RALMO) Water Vapour Mixing Ratio Measurements using a Radiosonde Trajectory Method

Shannon Hicks-Jalali[1*], R.J. Sica[1, 2], Alexander Haefele[2, 1] and Giovanni Martucci[2]

[1]*Department of Physics and Astronomy, The University of Western Ontario, London, Canada,* [*]*shicks26@uwo.ca*
[2]*Federal Office of Meteorology and Climatology, MeteoSwiss, Switzerland*

ABSTRACT

With only 50% downtime from 2007-2016, the RALMO lidar in Payerne, Switzerland, has one of the largest continuous lidar data sets available. These measurements will be used to produce an extensive lidar water vapour climatology using the Optimal Estimation Method introduced by Sica and Haefele (2016). We will compare our improved technique for external calibration using radiosonde trajectories with the standard external methods, and present the evolution of the lidar constant from 2007 to 2016.

1 INTRODUCTION

Water vapour is the dominant greenhouse gas and it plays a prominent role in atmospheric chemistry and dynamics. Water vapour distribution is controlled by and controls upper troposphere and lower stratosphere (UTLS) dynamics. Water vapour density is extremely variable both spatially and temporally and can exceed variations over 4 orders of magnitude between the ground and the tropical tropopause [1]. There are few long-term water vapour data sets with high enough accuracy and precision to provide the information necessary to discern cyclical and persistent behaviour. The RALMO has 9 years of measurements with an average of 50% uptime. This makes it uniquely capable of detecting long-term variations as well as diurnal, seasonal, and annual cycles. The RALMO is also supported with twice-daily radiosonde and sporadic lyman-α hygrometer soundings for measurement validation and redundancy. The RALMO water vapour mixing ratio measurements will be processed using the OEM introduced in [2].

In preparation for a multi-year water vapour mixing ratio climatology, it is first necessary to determine the evolution of the RALMO water vapour calibration factor. One cause of the change in the calibration factor is the accelerated deterioration of the water vapour photomultiplier tube (PMT) with respect to the nitrogen PMT [3].

For our purposes the calibration factor is defined as:

$$C_w = 0.781 \frac{\eta_{N_2}}{\eta_{H_2O}} \frac{O_{N_2}(z)}{O_{H_2O}(z)} \frac{\sigma_{N_2}(z)}{\sigma_{H_2O}(z)} \quad (1)$$

where 0.781 is the conversion value between the fraction of nitrogen molecules in air, $\eta_{\mathrm{N_2,H_2O}}$ is the system efficiency for the nitrogen and water vapour channels, $O_{\mathrm{N_2,H_2O}}(z)$ is the overlap function for both channels,and $\sigma_{\mathrm{N_2,H_2O}}(z)$ is the Raman cross-section for each molecular species.

2 METHODOLOGY

We have developed an improved lidar calibration method using Vaisala RS92 radiosondes based on the radiosonde tracking methods presented in [4] and [5]. However, unlike Whiteman et al. and Adam et al., we consider the wind speed and direction for each altitude bin. This calibration technique systematically accounts for the displacement of the radiosonde from the lidar, thereby increasing the validity

© The Authors, published by EDP Sciences. This is an open access article distributed under the terms of the Creative Commons Attribution License 4.0 (http://creativecommons.org/licenses/by/4.0/).

of the calibration when other instruments such as a microwave radiometer are not available. This paper presents a new calibration procedure that is tested on a single night's measurements. We are in the process of automating the procedure and applying it to 120 nighttime radiosonde flights.

All RS92 data is processed using the GCOS Reference Upper-Air Network (GRUAN) "gt92" processing tools [6] and only "FLEDT" files are used. One-minute lidar scans from the water vapour and nitrogen channels corresponding to $\pm$ 2 hours around the radiosonde launch are selected. Water vapour and nitrogen scans are selected based on nitrogen signal to noise ratios (SNRs) at 12 km. If the SNR of the nitrogen scan is below 1, the nitrogen scan and the corresponding water vapour scan are not used. Additionally, if the background in the nitrogen scan is higher than 0.01 photons, where the background is defined by the photocounts above 40 km, then both the nitrogen scan and water vapour scan are unusable. The radiosonde is interpolated onto the lidar altitude grid with a bin size of 3.75 meters. Molecular transmission is calculated using Nicolet [7] cross-sections for 407 nm and 387 nm. Number density is determined using radiosonde pressure and temperature.

The 2D air parcel trajectories are initialized from the radiosonde position at each altitude (Figure 1). The trajectories extend $\pm$ 2 hours in the direction of the wind, where their length is determined by the wind speed measured by GPS tracking. In most cases the air parcel trajectory does not pass directly over the field of view of the lidar; therefore, we define a region around the lidar where we assume that the mixing ratio is horizontally homogeneous. In order to maintain significant SNR values, we have chosen a 2 km radius around the lidar as the homogeneous region. The next step is to determine how long the air parcels remain inside the homogeneous region. The lidar measurements are integrated only for the period of time in

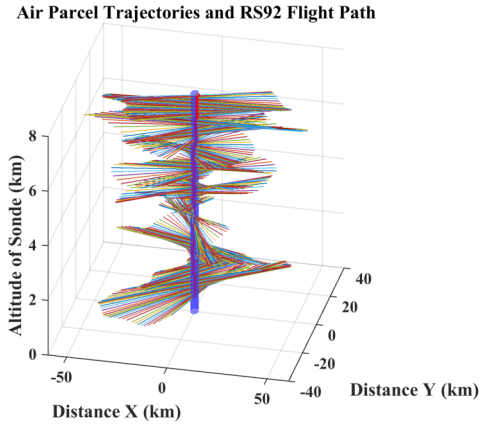

Figure 1: 4-hour 2D Air Mass Trajectories initialized from the radiosonde position (red line). The length of the trajectories is determined by the wind speed measured by the radiosonde GPS tracking. The blue cylinder represents the assumed horizontally homogeneous region around the lidar. We have chosen the radius to be 2 km.

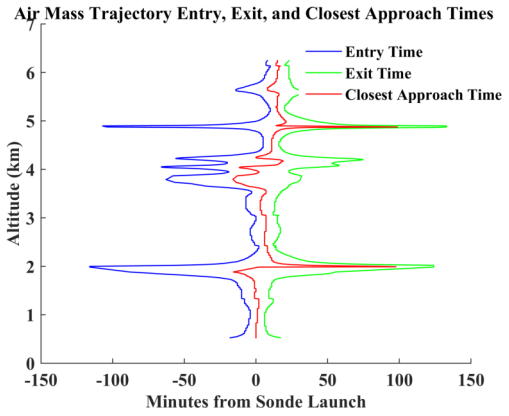

Figure 2: Air Mass trajectory entry (blue), exit (green), and closest approach (red) times. Entry and exit times correspond to the time when the air mass enters or exits the homogeneous region. The time of closest approach is the time at which the air mass is closest to the lidar. Integration times are determined by the exit and entry if the time spent inside the homogeneous region is less than 30 minutes. Otherwise, the integration time is 30 minutes around the time of closest approach.

which the air parcel remains inside the homogeneous cylinder (Figure 2), with a maximum of 30 minute integration in order to assume temporal homogeneity. Occasionally, due to wind direction, an air parcel does not pass through this region. In this case, there are no measurements for that particular altitude. Naturally, this process results in uneven integration times as a function of altitude. All pre-processing for saturation and background removal is done on a per scan basis before integration. After integration the mixing ratio is calculated using Eq. (2) where N_{H_2O} and N_{N_2} are the corrected water vapour and nitrogen photon counts, respectively, and T_{H_2O} and T_{N_2} are the molecular transmissions.

$$w = \frac{N_{H_2O}}{N_{N_2}} \cdot \frac{T_{H_2O}}{T_{N_2}} \tag{2}$$

We define the calibration region to be above 3 km to avoid signal saturation and using analog data. Additionally, we remove low SNR data by limiting the profiles to a region where the water vapour SNR is above 5. Finally, a standard least-squares fitting is done over the entire calibration region.

We then compare this trajectory method with the standard calibration method. The standard method integrates over a time interval that is constant with altitude after the radiosonde is launched. For our purposes, we chose to integrate for 30 minutes after the radiosonde is launched. All pre-processing of the data and data corrections are the same as the Trajectory Method.

3 RESULTS

A preliminary comparison of the standard calibration method with the trajectory method shows that the two produce very similar results (Figure 3). The standard method produces a calibration factor of 31.84 ± 0.09 and a regression coefficient of 0.99. The trajectory method produces a smaller calibration factor of 31.06 ± 0.10 and a regression coefficient of 0.99. The difference between the two calibration coefficients is statistically significant by a factor of 7 sigma. The larger fitting error of the trajectory method is likely due to the data gap at 3.8 km. This gap is caused by time of closest approach of the air parcels arriving before the launch when all of the data was masked by the vetting procedure prior to calibration. Differences between the two results are likely due to the trajectory method using data beyond the 30-minute window of the standard method. Figure 4 shows a 133% change in the water vapour content between 4 and 6 km over the 120 minutes of measurements.

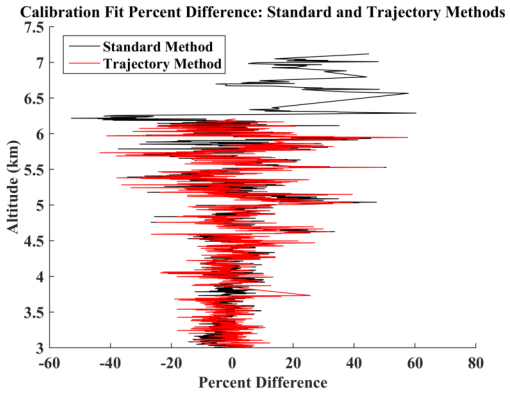

Figure 3: The percent difference between the RS92 mixing ratio profile and lidar calibrated profile using both the standard (black) and trajectory (red) methods.

4 CONCLUSIONS

Further comparisons are needed using all calibration nights to accurately determine the success of the trajectory method. These preliminary results suggest that the traditional method produces a larger fitting region due to larger SNR values at higher altitudes; however, the trajectory method produces a profile closer to the radiosonde (Figure 3).

Both the traditional and trajectory methods

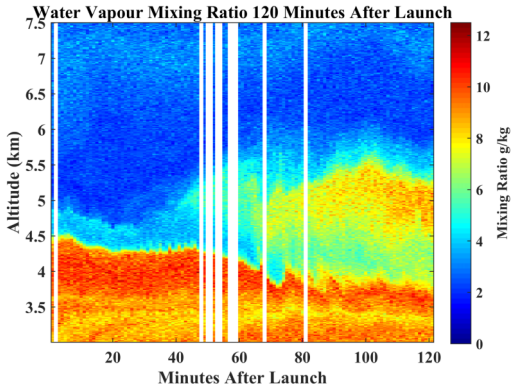

Figure 4: Lidar water vapour mixing ratio after RS92 launch. The white lines are scans that were filtered by the vetting procedure prior to calibration.

have limitations. The traditional method's results may be biased depending on the wind direction and speed. Low windspeeds allow the radiosonde to stay close to the lidar for the entire half-hour integration, in which case the traditional method would be valid. However, high wind speeds could carry the radiosonde farther from the lidar causing it to measure different air parcels thereby biasing the result. Without measuring the trajectory of the radiosonde, it is impossible to know whether or not the traditional method is acceptable. The trajectory method is primarily limited by short integration periods at higher altitudes due to high wind speeds. This could be compensated by allowing the radius of the homogeneous region to increase with altitude (i.e. using a cone instead of a cylinder); however, this remains a topic of further exploration.

We will expand upon this single-case result by testing the method over 120 calibration nights and will then determine a function representative of the calibration factor's evolution to use in the forthcoming water vapour mixing ratio OEM climatology.

ACKNOWLEDGEMENTS

This project has been supported by the Natural Sciences and Engineering Research Council (NSERC), the NSERC CREATE Training Program in Arctic Atmospheric Science and the Canadian Network for the Detection of Atmospheric Change, Canadian Space Agency, and MeteoSwiss.

References

[1] Andrew Gettelman and Michaela I Hegglin. Chapter 7: Upper Troposphere and Lower Stratosphere. *SPARC Report No.5*, volume 5, chapter 7. World Climate Research Program, 2010.

[2] R.J. Sica and Alexander Haefele. Retrievalof water vapor mixing ratio from a multiple channel Raman-scatter lidar using an optimal estimation method.*Applied Optics*, **55** (4), 2016.

[3] T. Dinoev et al. Raman Lidar for Meteorological Observations , RALMO Part 1: Instrument Description. *Atmos. Meas. Tech.*, 6:1329–1346, 2013.

[4] D.N. Whiteman et al. Analysis of Raman lidar and radiosonde measurements from the AWEX-Gfield campaign and its relation to Aqua validation.*JGR*,111 (November 2003):1–15, 2006

[5] M. Adam et al. Water vapor measurements by Howard university Raman lidar during the WAVES 2006 campaign. *Journal of Atmospheric and Oceanic Technology*, 27 (1):42-60, 2010

[6] R.J. Dirksen et al. Reference quality upper-air measurements: GRUAN data processing for the Vaisala RS92 radiosonde. *Atmos. Meas. Tech.*, 7(12):4463–4490, 2014

[7] Marcel Nicolet. On the molecular scattering in the terrestrial atmosphere : An empirical formula for its calculation in the homosphere.*Planetary and Space Science*, 32(11):1467–1468, 1984